

Poly(*p*-phenylene sulphide)/Liquid Crystalline Polymer Blends. I. Miscibility and Morphologic Studies

G. GABELLINI, M. B. de MORAES, and R. E. S. BRETAS*

Department of Materials Engineering, Universidade Federal de São Carlos, 13565-905 São Carlos, SP, Brasil.

SYNOPSIS

The miscibility in the melt and solid state of blends made of poly(*p*-phenylene sulphide) (PPS) with a liquid crystalline polymer (LCP) from DuPont was studied by polarized light optical microscopy (PLOM) and dynamic thermal mechanical analysis. Both techniques showed that the PPS and the LCP are immiscible in both states, and that the critical concentration for the formation of fibrils C^* , in this particular system, was located between 20 and 25 wt % LCP. The resultant blend morphology was studied by PLOM and scanning electron microscopy (SEM). It was observed that when LCP fibrils are formed in the PPS matrix, the PPS macromolecules will crystallize around the LCP fibrils by forming columnar layers called transcrystallites. These transcrystallites are the result of the LCP acting as a nucleating agent for the PPS, promoting heterogeneous nucleation. © 1996 John Wiley & Sons, Inc.

INTRODUCTION

Poly(*p*-phenylene sulphide) (PPS) is a high-temperature, high chemical resistant polymer, that has been widely used as an engineering thermoplastic. It can be employed in the construction of pump housings, tower packings, lamp sockets, microwave-compatible cookware, etc.¹ It also becomes a conductive polymer when doped with $AlCl_3$ and I_2 .² Besides being reinforced with glass and carbon fibers, it can be blended with liquid crystalline polymers (LCP) to produce high-performance composites.³ In all these applications, the determinant factor for achieving outstanding mechanical and electrical properties is usually the degree of crystallinity.

In the case of composites, for example, it is known that the presence of reinforcing glass, carbon, and aramid fibers affects the crystallization kinetics (and sometimes the final crystallinity) of the polymeric matrix;^{4,5} while these kinetics, in the case of LCP fibrils, can depend on the miscibility of the two polymers in the molten and solid states.^{6,7,8,9} In this regard we have observed that a polymer like poly-

etheretherketone (PEEK) that is miscible in the solid state with a LCP (HX4000, from DuPont) has its overall crystallization rate retarded by the presence of the LCP molecules; also, less perfect PEEK crystals and more perfect LCP domains are produced.⁹ The PEEK lateral and fold surface interfacial free energies, σ and σ_e , respectively, are modified by the presence of the LCP,⁹ and σ is found to decrease with the LCP increase. In other words, due to the miscibility of both components, the LCP rigid chains lower the lateral surface free energy that the PEEK macromolecules would expend on crystallization, resulting in more extended crystals. This morphology was confirmed by polarized light optical microscopy (PLOM).⁹

Another study, this time on the crystallization behavior of PPS with an LCP (Vectra, from Hoechst)⁷ has concluded that the nonisothermal crystallization temperature, T_c , and the equilibrium melting temperature, T_m^0 , of the PPS are not affected by the concentration of LCP, due to immiscibility of the two polymers in the molten state. These authors also found that, in the LCP range concentration studied (2 to 20 wt %), the LCP did not act as a nucleating agent for the PPS. However, no experimental data of miscibility on the melt state and no calculation of σ_e were reported to correlate with their findings.

* To whom correspondence should be addressed.

Therefore, to clarify the influence of the molten-state miscibility of PPS and a LCP on the PPS crystallization kinetics, we have undertaken this present study. The first part of this work will refer to the analysis of the miscibility of PPS and the LCP in the melt and solid states, and to the analysis of the resultant blend morphology. The second part will analyze the influence of this miscibility on the PPS crystallization kinetics and therefore on the values of σ and σ_e .¹⁰

EXPERIMENTAL

Materials

The PPS (Ryton V-1) utilized was from Phillips Petroleum Co., (USA), with density $\rho = 1.263 \text{ g/cm}^3$; the LCP was a polyester based on terephthalic acid, phenylhydroquinone, and hydroquinone (HX4000) from DuPont, (Delaware, USA) with density $\rho = 1.308 \text{ g/cm}^3$.

Blending

Before blending, both polymers were vacuum-dried at 115°C for 5 days. The injection molding of the samples (minitensile bars, ASTM D638) was done in an Arburg injection molding machine (model 221-55-250) using the following barrel temperatures: zones 1, 2 and 3, 360°C ; zone 4, 340°C . The mold was held at 60°C . Blends of 80/20, 60/40, 40/60, and 20/80 PPS/HX4000, on a weight percent basis, were prepared.

Miscibility Studies

Polymer/polymer miscibility can be studied by a variety of techniques, such as scanning electron microscopy (SEM), transmission electron microscopy (TEM), infrared (IR), small angle X-rays (SAXS), PLOM, and differential scanning calorimetry (DSC). SEM, TEM, IR, and SAXS are more accurate; they will resolve domains down to $0.001 \mu\text{m}$.¹¹ However, to study miscibility in the melt state with these techniques, the samples must be quenched, which is a difficult task when dealing with phase separation and crystallization of one (or both) of the components. PLOM is less accurate; it will resolve domains down to $1 \mu\text{m}$ only. However, in the melt state it gives relatively good results, especially when the components have different refraction indices or colors. In our case, the molten LCP fibrils are opaque and the molten PPS is transparent;

therefore, this miscibility can be investigated with some accuracy. DSC miscibility results are presented in Part II of this work.¹⁰

A polarized light optical microscope from Nikon and a hot stage (Linkam THMS600) were used. In order to simulate as nearly as possible the processing

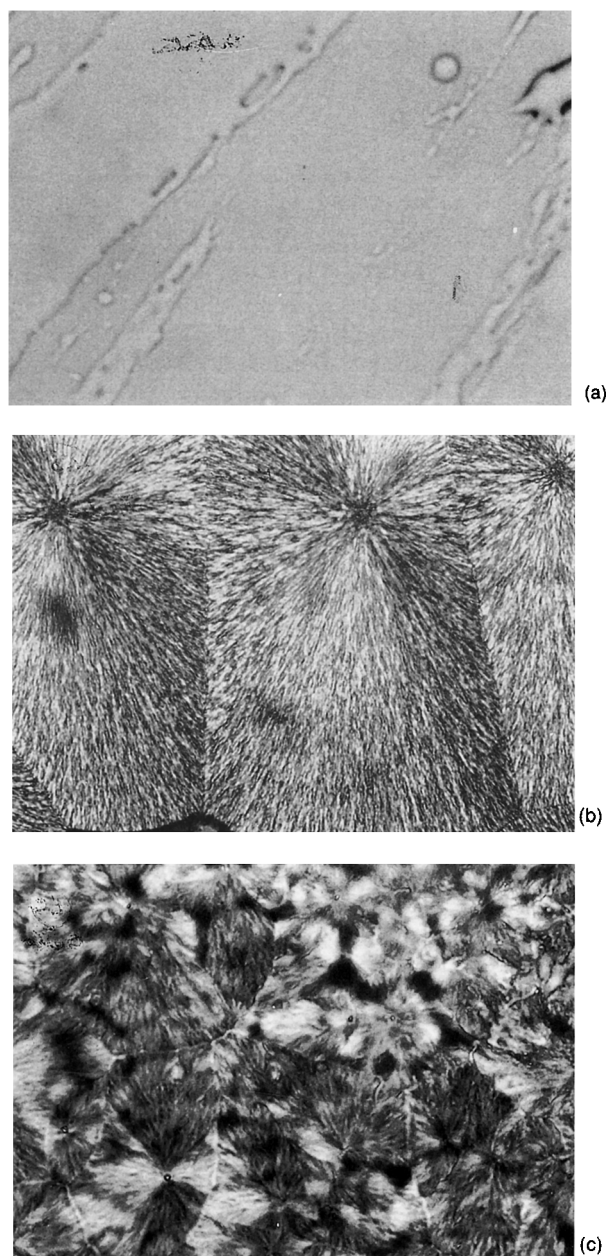


Figure 1 (a) Polarized light optical micrograph of a PPS/HX4000 97/3 blend at 330°C without shearing. Magnification: $50\times$. (b) Polarized light optical micrograph of pure PPS, at 25°C , without shearing. Magnification: $250\times$. (c) Polarized light optical micrograph of a PPS/HX4000 80/20 blend at 25°C , without shearing. Magnification: $400\times$.

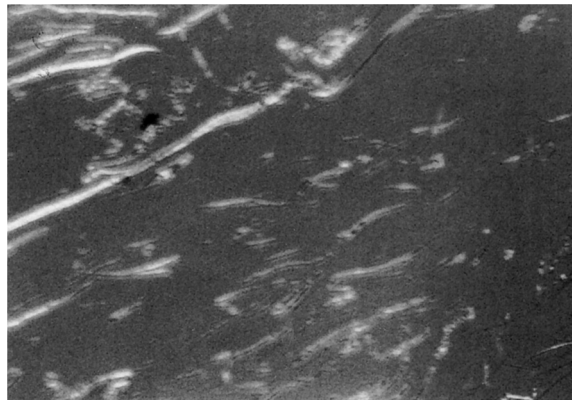


Figure 2 Polarized light optical micrograph of a PPS/HX4000 75/25 blend, at 330°C, after shearing. Magnification: 50 \times .

conditions, the blends were sheared in the melt state. First, the PPS powder was melted at 330°C. After complete melting, it was sheared with a microscope glass cover. The HX4000 was then added and mixed, and the blend was sheared again. After 10 min, the blend was cooled down to 250°C at a cooling rate of $-130^{\circ}\text{C}/\text{min}$ and maintained at this temperature for 20 min.

Miscibility in the solid state was determined by using a dynamic mechanical thermal analyzer (DMTA), from Polymers Lab, in the double cantilever bending mode at a frequency of 10 Hz, deflection of 64 μm and heating rate of $2^{\circ}\text{C}/\text{min}$. To obtain more thermodynamically stable samples, annealing was performed at 140°C, under N_2 for 48 h.

Morphologic Studies

To observe the morphology of the HX4000 in the PPS matrix and to correlate with composition, scanning electron micrographs of the central area of the minitensile bars were taken. The observed surfaces were perpendicular to the direction of the flow. (The microscope was a Carl Zeiss electron microscope, model DSM 940A.) These surfaces were obtained by breaking the samples in liquid N_2 .

RESULTS AND DISCUSSION

Miscibility in the Melt State

Figure 1(a) shows a micrograph of a PPS/HX4000 93/7 blend at 330°C after shearing. Neither the orientation of the PPS matrix nor the formation of LCP fibrils can be observed. At this concentration, miscibility of both polymers seems to occur. Even

when fibrils are not formed, the PPS morphology after crystallization can be affected by the LCP. This can be seen in Figures 1(b) and 1(c), which show a micrograph of pure PPS after complete crystallization (Fig. 1[b]) and a micrograph of an 80/20 blend, also after complete crystallization (Fig. 1[c]). It can be observed that pure PPS forms radial, finely textured spherulites with linear boundaries, while the 80/20 blend forms coarsely textured spherulites

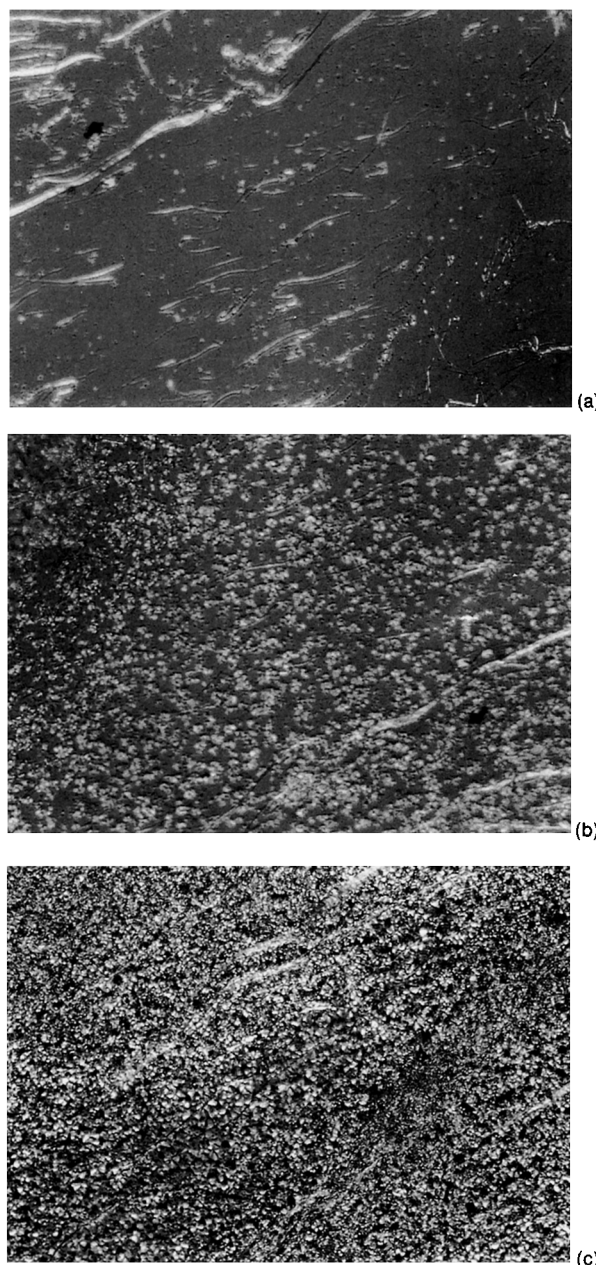


Figure 3 Polarized light optical micrograph of a PPS/HX4000 75/25 blend, at 250°C (magnification: 50 \times): (a) After 3 min. (b) After 5 min. (c) After 20 min.

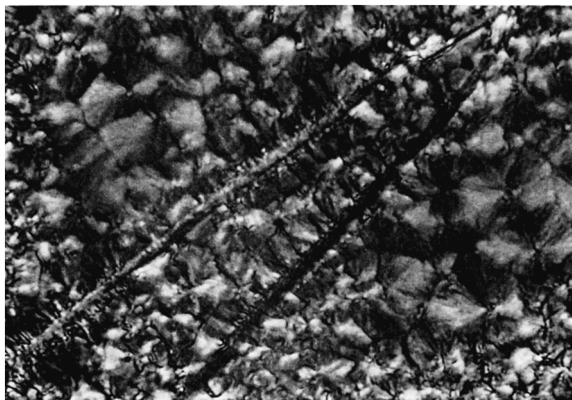


Figure 4 Polarized light optical micrograph of a PPS/HX4000 75/25 blend, at 250°C. Magnification: 200×.

with rounded boundaries. This spherulite coarsening could be due to the trapping of LCP molecules intraspherulitically during the crystal front growth; that is, the PPS growth rate probably outstrips the rate at which the LCP molecules can diffuse away from this growth front.¹²

A recent study on miscibility predictions for PPS¹³ showed that the presence of aromatic side groups in a polymer enhances its miscibility with PPS due to ring–ring π -electron interactions; also, exothermic heats of mixing are observed between the PPS model and compounds that contain carbonyl groups (aliphatic esters). However, aromatic ketones showed no interaction with the PPS model. From these observations, some specific interactions between PPS and the HX4000 should be expected.

Figure 2 shows a micrograph of a 75/25 PPS/HX4000 blend at 330°C, after shearing. It can be observed that the LCP forms birefringent fibrils in the PPS melt. This is an indication of immiscibility or partial miscibility of both polymers at this concentration in the melt state. After 10 min, the sample was cooled to 250°C, and the PPS began to crystallize. Figure 3(a) shows the surging of the PPS nuclei after 3 min, while Figure 3(b) shows the growing of the spherulites. After 20 min the PPS has completely crystallized, as shown in Figure 3(c). The central area of this last micrograph was magnified as shown in Figure 4. It can be observed that the PPS forms a transcrystalline columnar layer around the LCP fibrils. This transcrystallinity has been observed in thermoplastic/carbon fiber composites.¹⁴ Usually when a carbon fiber is embedded in a thermoplastic melt, it acts as a nucleating agent. If the surface of the fiber presents many nucleation sites, then spherulitic growth will be restricted in the lateral direction so that a columnar layer will develop. Thus, it seems that the LCP fibrils can induce the development of transcrystallinity in the PPS. It can also be observed that the formation of fibrils will occur only after a critical concentration C^* is attained, as already confirmed by other studies.¹⁵

Miscibility in the Solid State

The criteria for miscibility in the solid state were based on the study of the glass transition temper-

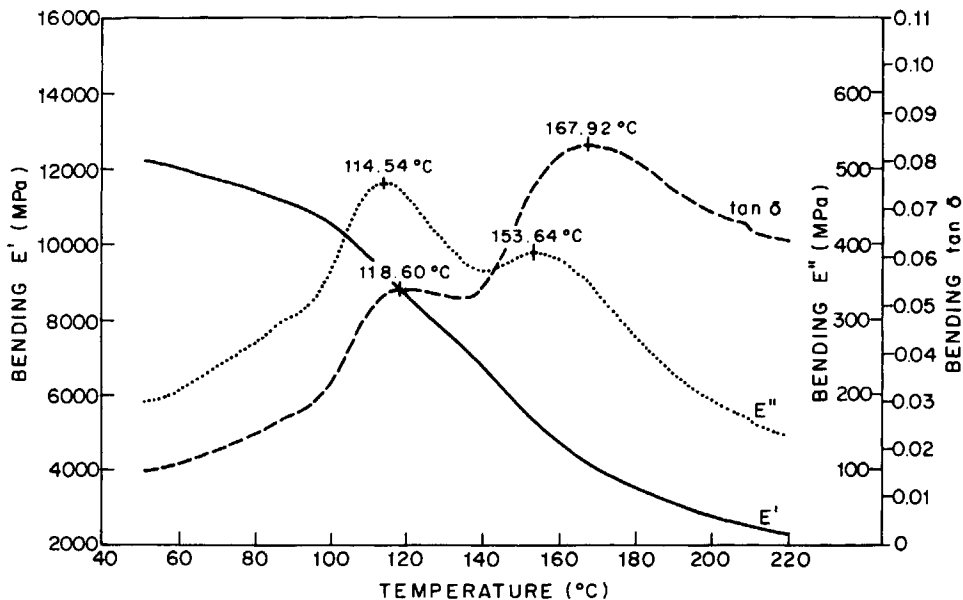


Figure 5 Typical dynamic mechanical thermal run of a PPS/HX4000 40/60 blend.

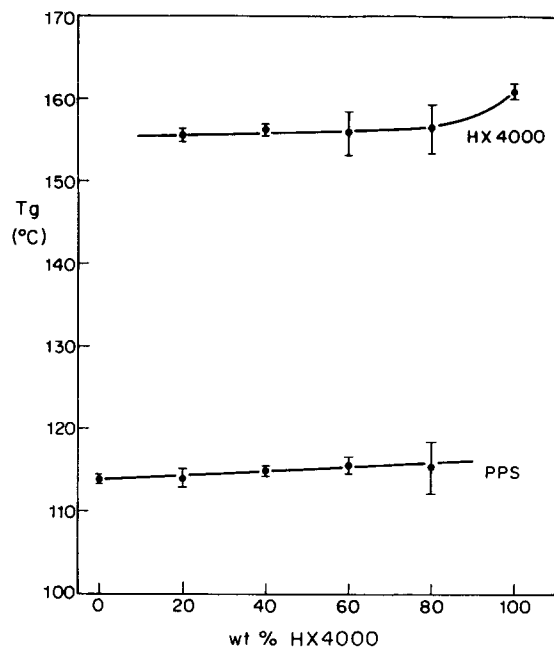


Figure 6 Glass transition temperature (T_g) as a function of composition, after annealing.

atures (T_g s) of the blends, by using DMTA. The T_g was taken as the temperature where a maximum in the loss modulus (E'') appears. If the blend shows only one T_g , then it can be stated that the amorphous parts of both polymers are miscible. If it shows two T_g s, then immiscibility or partial miscibility (depending on the closeness of both transitions) of the amorphous parts occurs. Figure 5 shows a typical DMTA run as a function of the temperature. Two well-defined E'' peaks can be observed. The first peak corresponds to the T_g of the PPS and the second to the T_g of the HX4000. Figure 6 shows these T_g s as a function of composition. Each value correspond to the average of two and sometimes three measurements. No increase in the storage modulus (E') was observed, indicating that cold crystallization did not occur.

It can be observed from Figure 6 that the T_g of the PPS in the blend does not change with composition. However, the T_g of the LCP decreases slightly with the decrease in the amount of LCP. Because the two T_g s are widely separated, the analysis can be more accurate. Thus it can be concluded that, in the solid state, the amorphous part of PPS is not miscible with the "amorphous" phase of the LCP. However, the "amorphous" part of the LCP seems to be slightly "plasticized." The observed slight reduction in T_g could be due to several reasons. For example, because this technique is based on mechanical response, if a blend has a dispersed phase

with a higher T_g than the continuous one, it will be difficult to measure precisely the T_g of the dispersed phase because the continuous one will already be soft and the mechanical response of the whole blend will no longer be accurate.¹⁶ This should be valid for blends with LCP concentrations up to approximately 50 wt %. Another possibility is related to the distribution of molecular weight of the LCP macromolecules. We know that if the LCP is polydisperse, the longer macromolecules preferentially will constitute the anisotropic phase.¹⁷ Therefore, if the LCP is disoriented, more dilute and smaller rigid molecules (amorphous part) could be plasticized by some of the smaller PPS macromolecules that were rejected during the PPS crystallization. However, it could be questioned that if the PPS macromolecules act as a plasticizing agent on the LCP ones, why is the inverse behavior not observed? The explanation could be that in the amorphous part, the PPS macromolecules, besides being tied to the PPS crystalline lamellae, are randomly oriented and entangled between themselves, making the diffusion of the LCP rigid molecules into them difficult. On the other hand, the LCP molecules in the amorphous part are also randomly oriented but not entangled, making it easier to diffuse the smaller PPS molecules into them. The result is an increase in the free volume and mobility of the LCP chains and a decrease in T_g . Then, within the experimental error, we can consider that the PPS/HX4000 blends are immiscible (or slightly miscible) in the solid state.

Morphologic Studies

Figure 7(a) shows a SEM micrograph of a PPS/HX4000 80/20 blend. It shows that the LCP forms droplets in the PPS matrix. Figure 7(b) shows a micrograph of a 60/40 blend; this time the LCP has formed fibrils. In Figure 7(c), a 40/60 blend, and Figure 7(d), a 20/80 blend, the LCP in both blends has formed fibrils. Whether or not fibrils would arise will depend (besides other factors, such as the extruder die L/D ratio and interfacial tension) on the viscosity ratio, η_d/η_m , where η_d is the viscosity of the disperse phase and η_m is the viscosity of the matrix, and on the attainment of the critical weight concentration C^* .¹⁸ Usually, when this viscosity ratio is less than 1, droplets or a fine dispersion (fibrils) of the disperse phase can result. If this ratio is higher than 1, a coarse droplet dispersion could result that would be extended only in strong elongational flows. In our systems, depending on the volume concentration, the HX4000 will be the disperse or the matrix phase. We already know that the viscosity of

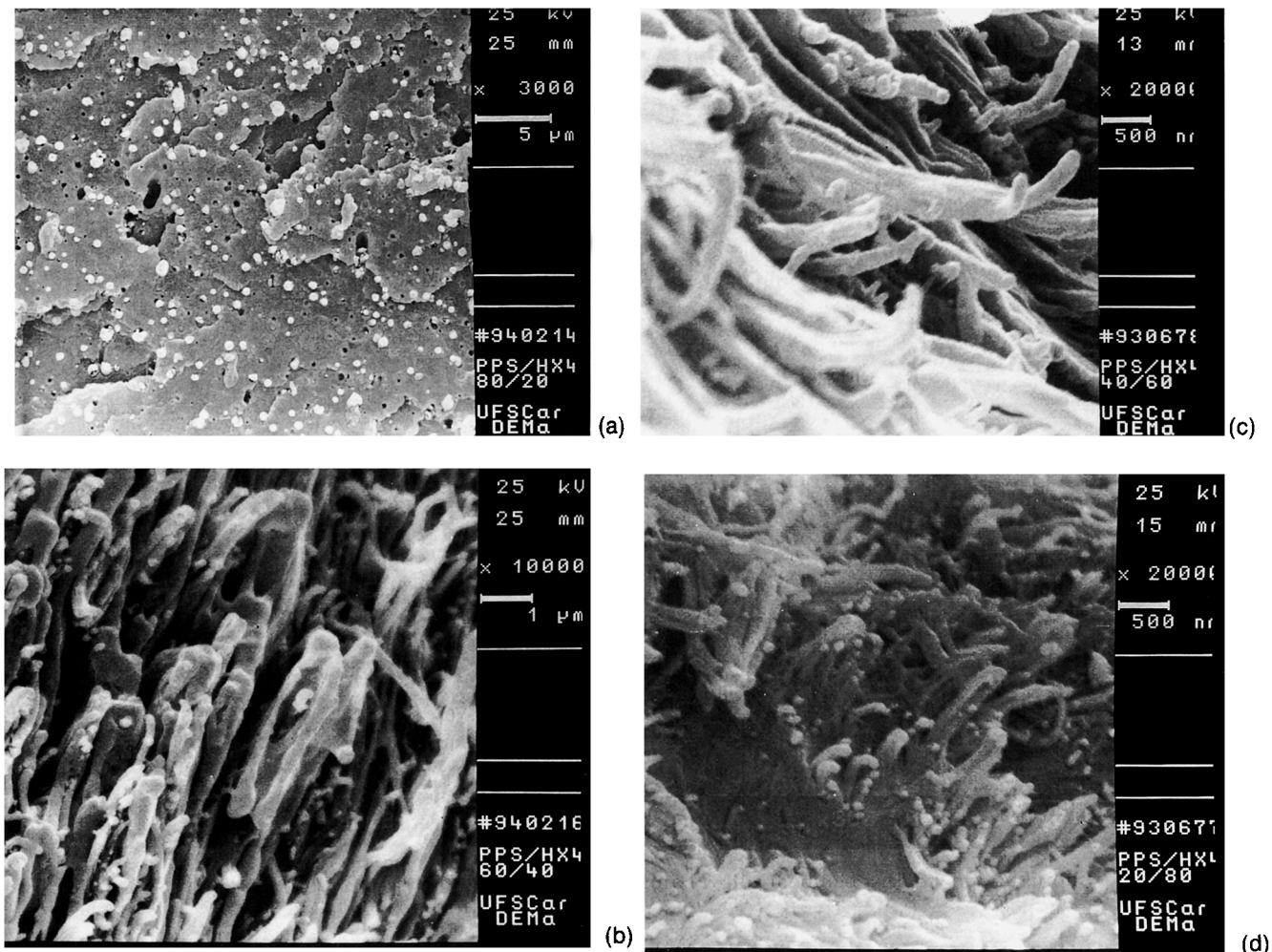


Figure 7 Scanning electron micrographs of PPS/HX4000 blends: (a) 80/20 blend (magnification: 3,000 \times); (b) 60/40 blend (magnification: 10,000 \times); (c) 40/60 blend (magnification: 20,000 \times); (d) 20/80 blend (magnification: 20,000 \times).

the HX4000, η_{HX4000} , is lower than the viscosity of the PPS, η_{PPS} , at all shear rates.¹⁵ Therefore, at low volume concentrations of HX4000, $\eta_d = \eta_{\text{HX4000}}$ and $\eta_m = \eta_{\text{PPS}}$. Then $\eta_d/\eta_m < 1$ and fibrils could arise. At high volume concentrations of HX4000, $\eta_d = \eta_{\text{PPS}}$, $\eta_m = \eta_{\text{HX4000}}$ and $\eta_d/\eta_m > 1$. Probably, fibrils will form only if a strong extensional deformation occurs.

Both polymers have approximately the same density; then, the weight fraction can be considered similar to the volume fraction. From the micrographs, we can observe that at 40 wt % LCP (or approximately 40 vol % LCP), fibrils were already formed. This means that in this particular system, C^* is between 20 and 40 wt % LCP; once this concentration is attained, if the viscosity ratio and deformational flow are appropriate, fibrils will form. Between 20 and approximately 50 wt % HX4000,

these two last-mentioned parameters were appropriate because a fibrillar morphology was obtained. However, at concentrations above 50 wt % HX4000, fibrils were formed due to the existence of high extensional deformation in the constricted central area of the minitensile bars.

Other observations regarding the morphology can also be made: at a 40 wt % LCP concentration, there is low adhesion between fibrils and matrix; and at 60 and 80 wt % LCP concentrations, no distinction between matrix and fibrils can be made.

CONCLUSIONS

From these preliminary studies some conclusions can be drawn:

1. From the PLOM and SEM data, it can be observed that the necessary critical concentration for the formation of fibrils, C^* , in this particular system, is located between 20 and 25 wt % HX4000. Once C^* is attained, if the viscosity ratio and deformational flow are appropriate, fibrils will form.
2. In the melt state, at low concentrations (3 wt %), the LCP is miscible (at least visually) with the PPS; at higher concentrations (25 wt %), the LCP is already immiscible with the PPS.
3. When LCP fibrils are formed in the PPS matrix, the matrix will crystallize around these fibrils by forming columnar layers called transcrystallites. This transcrystallinity is the result of the HX4000 fibrils acting as nucleating agents for the PPS, promoting heterogeneous nucleation. Comparing this work with the that of Minkova and colleagues,⁷ we can conclude that probably, at the LCP range concentration studied by them (2 to 20 wt %), the LCP did not form fibrils and then did not act as a nucleating agent for the PPS.

The authors express their gratitude to FAPESP (92/0990-2) and the Volkswagen Foundation (I/69 693), Germany, for their financial support, and to Dr. Donald G. Baird for the preparation of the samples.

REFERENCES

1. J. M. Charrier, *Polymeric Materials and Processing*, Hanser Publishers, New York, 1991.
2. R. E. S. Bretas, M. C. B. de Jesus, and G. Lunardi, *J. Mat. Sci.*, **27**, 2345 (1992).
3. D. G. Baird, T. Sun, D. S. Done and R. Ramanathan, *Am. Chem. Soc., Div. Polym. Chem., Polym. Prepr.*, **30**, 546 (1989).
4. V. L. Shingankuli, J. P. Jog, and V. M. Nadkarni, *J. Appl. Polym. Sci.*, **36**, 335 (1988).
5. C. Auer, G. Galinka, T. H. Krause, and G. Hinrichsen, *J. Appl. Polym. Sci.*, **51**, 407 (1994).
6. E. Martuscelli, *Polym. Eng. Sci.*, **24**, 563 (1984).
7. L. Minkova, M. Paci, M. Pracella, and P. Magagnini, *Polym. Eng. Sci.*, **32**, 57 (1992).
8. R. E. S. Bretas and D. G. Baird, *Polymer*, **33**, 5233 (1992).
9. B. de Carvalho and R. E. S. Bretas, *J. Appl. Polym. Sci.*, **55**, 233 (1995).
10. G. Gabellini and R. E. S. Bretas, *J. Appl. Polym. Sci.*, submitted.
11. L. A. Utracki, *Polymer Alloys and Blends: Thermodynamics and Rheology*, Hanser Publishers, New York, 1989.
12. J. P. Runt and L. M. Martynovitz, in *Multicomponent Polymer Materials*, Adv. Chem. Ser., D. R. Paul and L. H. Sperling, Eds., ACS, Washington D. C., 1986, Chap. 7.
13. C. J. T. Landry and D. M. Teegarden, *J. Polym. Sci., Part B: Polym. Phys.*, **32**, 125 (1994).
14. W. S. Carvalho and R. E. S. Bretas, *Eur. Polym. J.*, **26**, 817 (1990).
15. B. Carvalho, G. Gabellini, and R. E. S. Bretas, *Poli-meros: Ciencia e Tecnologia*, V, 2, **31** (1995).
16. A. Morales and R. E. S. Bretas, *Eur. Polym. J.*, to appear.
17. "High Performance Polymers and Composites", Encyclopedia Reprint Series, J. I. Kroschwitz, Ed., John Wiley and Sons, New York, 1991.
18. R. E. S. Bretas, D. Collias, and D. G. Baird, *Polym. Eng. Sci.*, **34**, 1492 (1994).

Received January 12, 1995

Accepted July 31, 1995